The neural computation of human goal-directed behaviors in complex motivational states

Anne Saulin[1*], Ulrike Horn[2], Martin Lotze[3], Jochen Kaiser[4], & Grit Hein[1*]

[1] Translational Social Neuroscience Unit, Department of Psychiatry, Psychosomatics, and Psychotherapy, University of Würzburg, Würzburg, Germany.
[2] Max Planck Institute for Human Cognitive and Brain Sciences, Leipzig, Germany.
[3] Functional Imaging Unit, Institute of Diagnostic Radiology and Neuroradiology, University of Greifswald, Greifswald, Germany.
[4] Institute of Medical Psychology, Faculty of Medicine, Goethe University, Frankfurt am Main, Germany.

***corresponding authors:**
Anne Saulin, Saulin_A@ukw.de
Grit Hein, Hein_G@ukw.de

Abstract

Because the motives behind goal-directed behaviors are often complex, most behaviors result from the interplay between different motives. However, it is unclear how this interplay between multiple motives affects the neural computation of goal-directed behaviors. Using a combination of drift-diffusion modeling and fMRI, we show that the interplay between different social motives changes initial preferences for prosocial behavior before a person makes a behavioral choice. This increase in preferences for the prosocial choice option was tracked by neural responses in the bilateral dorsal striatum, which in turn lowered the amount of information necessary for choosing prosocial behavior. We obtained these results using a paradigm in which each participant performed the same behavior based on different, simultaneously activated motives, or based on each of the motives separately. Thus, our findings provide a model of behavioral choice computation in complex motivational states, i.e., the motivational setting that drives most goal-directed human behaviors.

Introduction

All goal-directed behaviors are incited by motives, which can be complex. Documenting this motivational complexity, many animal (Jennings et al., 2013; Kennedy & Shapiro, 2009) and most human behaviors are driven by multiple motives that are active at the same time, and affect each other (Engel & Zhurakhovska, 2016; Hughes & Zaki, 2015; Jagers, Linde, Martinsson, & Matti, 2017; Kruglanski et al., 2018; Lewin, Cartwright, & Price, 1951; Takeuchi, Bolino, & Lin, 2015; Terlecki & Buckner, 2015). Consequently, goal-directed behaviors most commonly originate from the interplay between different motives and cannot be explained by one “motivational force” alone. Thus, to understand and predict goal-directed behaviors, it is crucial to elucidate the neuro-computational mechanisms through which multiple interacting motives affect behavioral choice processes.

So far, most previous studies have investigated one specific motive at a time, providing single-motive based models of behavior. Animal studies, for example, have examined basic motivational states (e.g., elicited by food rewards) (Cromwell & Schultz, 2006; Palmiter, 2008; Wang, Miura, & Uchida, 2013). On the neural level, the processing of such basic motivational states and impact on behavioral choices (e.g., place preferences) (Jennings et al., 2013) have been linked to dopaminergic neurons in the striatum (Kim & Im, 2018; Robinson, Sotak, During, & Palmiter, 2006; Salamone & Correa, 2012). In line with these results, human neuroscience studies have shown that the striatum is involved in the processing of different individual motives, as well as motivated choice behaviors, both in the social (Báez-Mendoza & Schultz, 2013; Bhanji & Delgado, 2014) and non-social domain (Salamone et al., 2016; Shohamy, 2011). Together, this previous work has provided insights into the neural underpinnings of individual motivational processes. However, the interplay between different motives and its impact on the neural computation of behaviors remains poorly understood.

To address this issue, we developed a paradigm in which participants made the same choices based on different, simultaneously activated motives, or based on each of the motives separately. In combination with fMRI and drift-diffusion modelling, this paradigm allowed us to specify how the interplay between different motives affects individual components of neural choice computation, compared to computation of the same choice in a simple motivational state (i.e., driven by only one of the two motives).

We studied the interplay between different motives in a social choice paradigm in which participants repeatedly had the choice between a prosocial and an egoistic option. Inspired by an influential model of prosocial motivations (Batson, Ahmad, & Stocks, 2011), we induced two key

motives that incite prosocial behavior - the empathy motive, defined as the affective response to another person's misfortune (Batson, Turk, Shaw, & Klein, 1995; Hein, Morishima, Leiberg, Sul, & Fehr, 2016; Lamm, Decety, & Singer, 2011), and the reciprocity motive, defined as the desire to reciprocate perceived kindness with a kind behavior (Gouldner, 1960; Hein et al., 2016; McCabe, Rigdon, & Smith, 2003). The two motives were induced separately (single-motive conditions) and simultaneously (multi-motive condition). After inducing the motives, the participants performed a choice task in which they could choose between a prosocial option (allocate money to another individual at a cost to themselves) and an egoistic option (allocate money to themselves at a cost to another individual) (**Fig. 1A**). Importantly, the choice task was the same regardless of the motive-induction condition. This approach allowed us to assess how a person computes a choice driven by only one motive, and how the same person computes the same choice in a complex motivational state, i.e., driven by the interplay between the different simultaneously activated motives.

We used hierarchical drift-diffusion modeling (HDDM) (Vandekerckhove, Tuerlinckx, & Lee, 2011; Wiecki, Sofer, & Frank, 2013) to investigate which aspects of the choice computation are altered by the interplay between the two motives. Drift-diffusion models (DDMs) characterize how noisy information is accumulated to select a choice option (**Fig. 1B**) based on three different parameters (the *v*, *z* and *a* parameters) (Forstmann, Ratcliff, & Wagenmakers, 2016; Ratcliff, Smith, Brown, & McKoon, 2016). The *v*-parameter describes the speed at which information is accumulated in order to choose one of the options, i.e., the efficiency of the choice process itself. The *z*-parameter reflects the initial choice preference, i.e., the degree to which an individual prefers one of the choice options prior to making the choice. Thus, in contrast to the *v*-parameter, which models the choice process itself, the *z*-parameter models the individual preferences with which a person enters the choice process. For example, if a person has a strong initial preference for prosocial choices (reflected by a large value of the parameter *z*), the starting point of the choice computation is located closer to the prosocial choice boundary, and thus, this person is more likely to choose the prosocial option. The third component, parameter *a*, quantifies the amount of information that is required to choose one of the options. We modeled these three parameters (*v, z*, and *a*) for choices that were driven by the combination of the two motives, and for the same choices that were driven by each of the motives separately. This allowed for direct comparisons between the parameters of choices driven by multiple motives and parameters of the respective choices driven by the single motives.

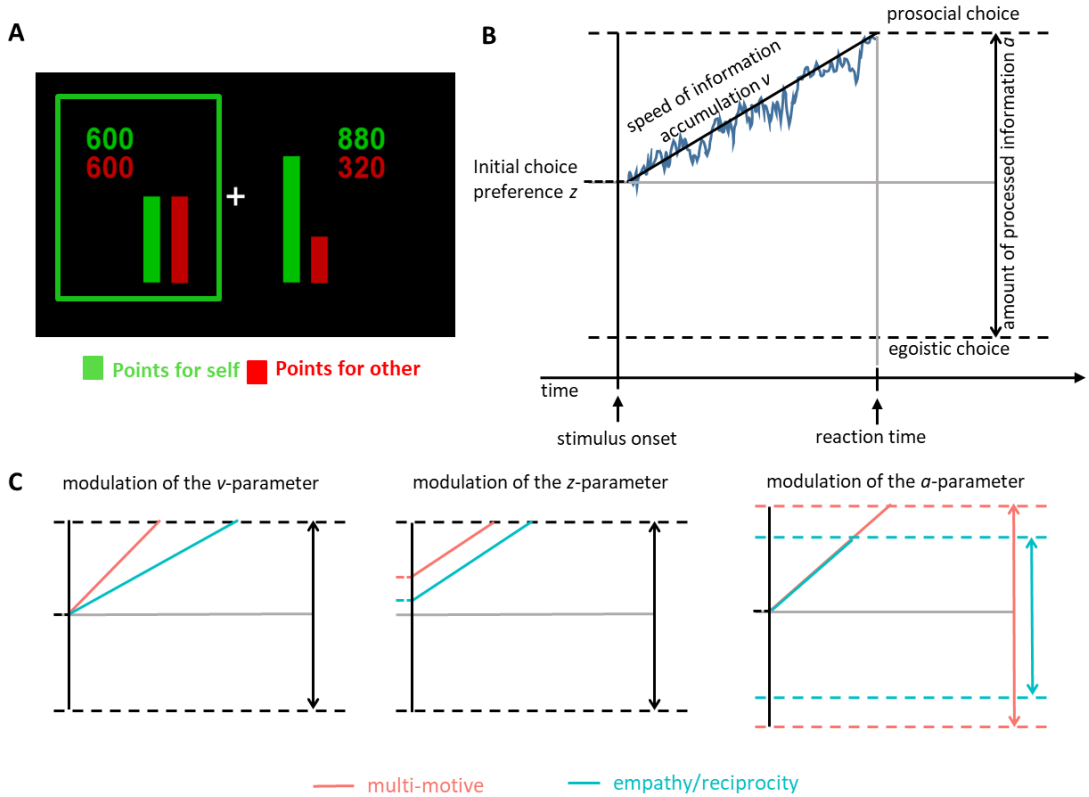

Figure 1. Example of point allocation during the choice task, schematic illustration of the drift-diffusion model and hypotheses regarding the impact of different drift-diffusion parameters on the choice process in multi-motive and single-motive conditions. **(A)** Participants chose between a prosocial and an egoistic option to allocate points to themselves (in this example shown in green) and a partner (in this example shown in red). Colors were counter-balanced across participants. In this example trial, the participant chose the prosocial option, which maximized the outcome of the partner at a cost to the participant (green box). **(B)** The drift-diffusion model conceptualizes the choice process as noisy accumulation of information (squiggly blue line). This process can be characterized in terms of the speed of information accumulation (*v*-parameter), the initial preference for one of the choice options (*z*-parameter), and the amount of processed information before a choice is made (*a*-parameter). Once the accumulated information reaches either boundary, the choice is made (upper boundary = prosocial choice; lower boundary = egoistic choice). **(C)** An enhancement of prosocial choice frequency in the multi-motive condition (red) compared to the single motive conditions (i.e., the empathy or the reciprocity condition; blue) may result from an increased speed of information accumulation (*v*-parameter; left panel), and/or an increased initial preference for a prosocial choice (*z*-parameter; middle panel). On average, the amount of relevant processed information (*a*-parameter) may be higher in the multi-motive condition compared to the single motive conditions (right panel).

Human motivation models (Kruglanski et al., 2018; Lewin et al., 1951) suggest that the interplay between the different motives generates a novel motivational state that cannot be explained by the difference between the single motives involved. This novel motivational state may facilitate the choice of the prosocial option. In this case, we should observe an increase in prosocial behavior in the multi-motive condition compared to the single-motive conditions that cannot be explained by the difference between the single-motive conditions. According to the DDM, such multi-motive facilitation of prosocial

choices could originate A) from an increased speed of information accumulation (*v*-parameter; Fig. 1C, left panel (Flagan, Mumford, & Beer, 2017; Janczyk & Lerche, 2019; Krajbich, Hare, Bartling, Morishima, & Fehr, 2015)), B) from an enhancement of participants' initial preference to choose the prosocial option (*z*-parameter; Fig. 1C, middle panel; (Chen & Krajbich, 2018; Mulder, Wagenmakers, Ratcliff, Boekel, & Forstmann, 2012; Toelch, Panizza, & Heekeren, 2018)), or C) from an enhancement of the *v*- as well as the *z*-parameter in the multi-motive condition, compared to the single-motive condition

Alternatively, it is possible that the multi-motive interplay impedes the choice of the prosocial option (and thus fosters egoistic choices), reflected by a decline of prosocial choices, the *v*-parameter, the *z*-parameter, or both parameters in the multi-motive condition compared to the single-motive conditions. Moreover, in the multi-motive condition, participants are required to process two motives simultaneously, in addition to the trial-by-trial information about the point allocations (which was constant across all conditions because participants performed the identical choice task). The additional motive-related informational load may increase the *a*-parameter in the multi-motive condition compared to the single-motive conditions. The resulting increase in the prosocial choice boundary may impede the prosocial choice process, and thus, lower the frequency of prosocial choices (**Fig.1C**, right panel).

During the study, participants were paired with four partners (confederates of the experimenter). In the empathy condition, the participants repeatedly observed one of the confederates (the empathy partner) receiving painful shocks in a number of trials, a situation known to elicit an empathic response (Batson et al., 1995; Hein et al., 2016; Lamm et al., 2011) (see Methods for details). The reciprocity motive is defined as the desire to reciprocate perceived kindness with kind behavior (Gouldner, 1960; Hein et al., 2016; McCabe et al., 2003). Therefore, in the reciprocity condition, we activated the reciprocity motive by instructing one of the confederates (the reciprocity partner) to give up money in several trials to save the participant from painful shocks (Hein et al., 2016). In the multi-motive condition, the participants repeatedly observed how one of the confederates (the multi-motive partner) received painful shocks and also gave up money to spare the participant from painful shocks. No motive was induced towards a fourth confederate (baseline partner, see STAR Methods for details).

Importantly, the number of painful shocks received by the participants was identical across all conditions. By equalizing the frequency of painful shocks, we ensured that all motive-induction

conditions contained the same number of aversive events. To assess the success of the motive-induction procedures, the participants completed emotion ratings in which they indicated how they felt in each trial of the induction procedure.

After the motive inductions, participants performed a social choice task inside the fMRI scanner. In each trial of this choice task, they allocated money to themselves and one of the partners (**Fig. 1A**) and could choose between maximizing the other person's monetary payoff by reducing their own (prosocial choice) and maximizing their own payoff at a cost to the partner (egoistic choice). Depending on the type of partner the participants faced in the choice task, there were four conditions – the empathy condition, the reciprocity condition, the multi-motive condition, and the baseline condition.

Results

During the empathy induction, participants indicated how they felt after observing the person in pain. During the reciprocity induction, they indicated how they felt after receiving a favor from the other person. In the multi-motive condition, participants provided both of these ratings. The results of linear mixed models (lmms) showed that the induction ratings in the motive conditions were significantly higher than those in the baseline condition ($\chi^2 = 515.15$, $P < .000001$). There were no significant differences in the induction ratings between the motive conditions ($\chi^2 = 0.14$, $P = .93$). The induction ratings in the motive conditions were significantly associated with the frequency of prosocial choices ($\chi^2 = 6.38$, $P = .01$). This effect held to a comparable extent across all three motive conditions (motive condition $\times$ rating interaction, $\chi^2 = 3.61$, $P = .16$). Specifically, the two single-motive conditions yielded similar induction ratings ($\chi^2 = 0.23$, $P = .64$) and had a comparable effect on the frequency of prosocial choices ($\chi^2 = 4.77$, $P = .03$, condition $\times$ rating interaction, $\chi^2 = 2.06$, $P = .15$).

The frequency of prosocial choices was significantly higher (lmm $\chi^2 = 11.47$, $P = .0007$) and reaction times significantly faster (lmm $\chi^2 = 10.31$, $P = .001$) in the motive conditions compared to the baseline condition. There were no differences in reaction times for prosocial choices between the motive conditions (lmm $\chi^2 = 0.80$, $P = .67$). The frequency of empathy-based and reciprocity-based prosocial choices was comparable (lmm $\chi^2 = 2.56$, $P = .11$), as was the frequency of prosocial choices between the multi-motive condition and the empathy condition (lmm $\chi^2 = 0.05$, $P = .82$). However, the multi-motive condition yielded significantly more prosocial choices compared to the reciprocity condition (lmm $\chi^2 = 3.64$, $P = .05$).

Note that the increase in prosocial choices in the multi-motive condition compared to the reciprocity condition was observed although the motives were induced with equal strength (no difference in induction ratings and frequency of prosocial choices between the motive conditions), and had a comparable effect on prosocial choices.

To clarify this effect, we calculated the percent change in prosocial choices in the multi-motive condition relative to each single motive condition

$$\Delta prosoc_{\text{multi-motive/reciprocity}} = \frac{prosoc_{\text{multi-motive}} - prosoc_{\text{reciprocity}}}{prosoc_{\text{reciprocity}}} \times 100$$

$$\Delta prosoc_{\text{multi-motive/empathy}} = \frac{prosoc_{\text{multi-motive}} - prosoc_{\text{empathy}}}{prosoc_{\text{empathy}}} \times 100$$

where $prosoc_{\text{multi-motive}}$ equals the frequency of the prosocial choices in the multi-motive condition, $prosoc_{\text{reciprocity}}$ equals the frequency of prosocial choices in the reciprocity condition, and $prosoc_{\text{empathy}}$ equals the frequency of prosocial choices in the empathy condition.

The percent change of the multi-motive condition relative to reciprocity was significantly positive ($t(32) = 2.07$, $P = .047$, $\Delta prosoc_{\text{multi-motive/reciprocity}} = 8.61 \pm 4.17$ ($M \pm SEM$)), demonstrating that prosocial choices were enhanced when reciprocity was combined with empathy, relative to reciprocity alone. The percent change in the multi-motive condition relative to the empathy condition was not significantly different from zero ($t(32) = 0.42$, $P = .674$, $\Delta prosoc_{\text{multi-motive/empathy}} = 1.05 \pm 2.47$ ($M \pm SEM$)), indicating that the simultaneous activation of the reciprocity motive did not enhance the empathy motive.

In the next step, we used hierarchical drift-diffusion modeling (HDDM) (Vandekerckhove et al., 2011; Wiecki et al., 2013) to reveal the mechanism behind the change in prosocial behavior in the multi-motive condition that we observed relative to the reciprocity condition. We estimated the three aforementioned DDM parameters (*v, z, a*) for every condition and participant. Based on the hypotheses depicted in **Fig. 1C**, we tested whether the observed percent change in the multi-motive condition can be explained by an increase in the speed of information accumulation (*v*-parameter, **Fig. 1C**, left panel), and/or an increase in initial prosocial choice preferences (*z*-parameter, **Fig. 1C**, middle panel). Additionally, we tested whether the induction of both motives enhanced the amount of information that participants considered during the choice process, relative to the two single-motive conditions (*a*-parameter, **Fig, 1C**, right panel).

Testing the first hypothesis (**Fig. 1C**, left panel), we found no significant difference between the motive conditions in the speed of information accumulation (lmm $\chi^2 = 2.65$, P = .27). Confirming this finding, there was no significant percent change in *v*-parameters in the multi-motive condition, relative to the reciprocity or the empathy condition ($\Delta v_{\text{multi-motive/reciprocity}} = \frac{v_{\text{multi-motive}} - v_{\text{reciprocity}}}{v_{\text{reciprocity}}} \times 100 = -16.22 \pm 45.84$ % (*M* ± *SEM*), $t(32) = -0.35$, P = .72; $\Delta v_{\text{multi-motive/empathy}} = \frac{v_{\text{multi-motive}} - v_{\text{empathy}}}{v_{\text{empathy}}} \times 100 = 155.57 \pm 142.40$ % (*M* ± *SEM*), $t(32) = 1.09$, P = .28). This result showed that the speed of information accumulation, i.e., the efficiency of the choice process itself, was not affected by the combination of the two motives, relative to the single-motive conditions.

Testing the second hypothesis (**Fig. 1C**, middle panel), we observed a significant increase in initial prosocial choice preferences in the multi-motive condition compared to the reciprocity condition (lmm $\chi^2 = 4.78$, P = .03) (**Fig. 2A**), but not compared to the empathy condition (lmm $\chi^2 = 0.20$, P = .66). The percent change in the *z*- parameter of the multi-motive condition relative to the reciprocity condition was significantly positive ($z_{\text{multi-motive/reciprocity}} = \frac{z_{\text{mulit-motive}} - z_{\text{reciprocity}}}{z_{\text{reciprocity}}} \times 100 = 5.55 \pm 2.14$ % (*M* ± *SEM*), ($t(32) = 2.59$, P = .01), whereas there was no such effect relative to empathy ($\Delta z_{\text{multi-motive/empathy}} = \frac{z_{\text{multi-motive}} - z_{\text{empathy}}}{z_{\text{empathy}}} \times 100 = 2.35 \pm 2.51$ % (*M* ± *SEM*), ($t(32) = 0.94$, P = .36).

In addition, we had hypothesized that the combination of the two motives may increase the amount of information that was processed to reach a decision (captured by the *a*-parameter; **Fig. 1C,** right panel). Supporting this hypothesis, the *a*-parameter was higher in the multi-motive condition compared to the reciprocity condition (lmm $\chi^2 = 4.76$, P = .03), but not compared to the empathy condition (lmm $\chi^2 = 2.21$, P = .14). Correspondingly, there was a significantly positive percent change in *a*-parameters in the multi-motive condition relative to the reciprocity condition ($\Delta a_{\text{multi-motive/reciprocity}} = \frac{a_{\text{multi-motive}} - a_{\text{reciprocity}}}{a_{\text{reciprocity}}} \times 100 = 7.76 \pm 3.30$ % (*M* ± *SEM*), $t(32) = 2.35$, P = .02). The percent change in *a*-parameters in the multi-motive condition relative to the empathy condition was marginally larger than zero ($\Delta a_{\text{multi-motive/empathy}} = \frac{a_{\text{multi-motive}} - a_{\text{empathy}}}{a_{\text{empathy}}} \times 100 = 6.94 \pm 3.58$ % (*M* ± *SEM*), $t(32) = 1.94$, P = .06).

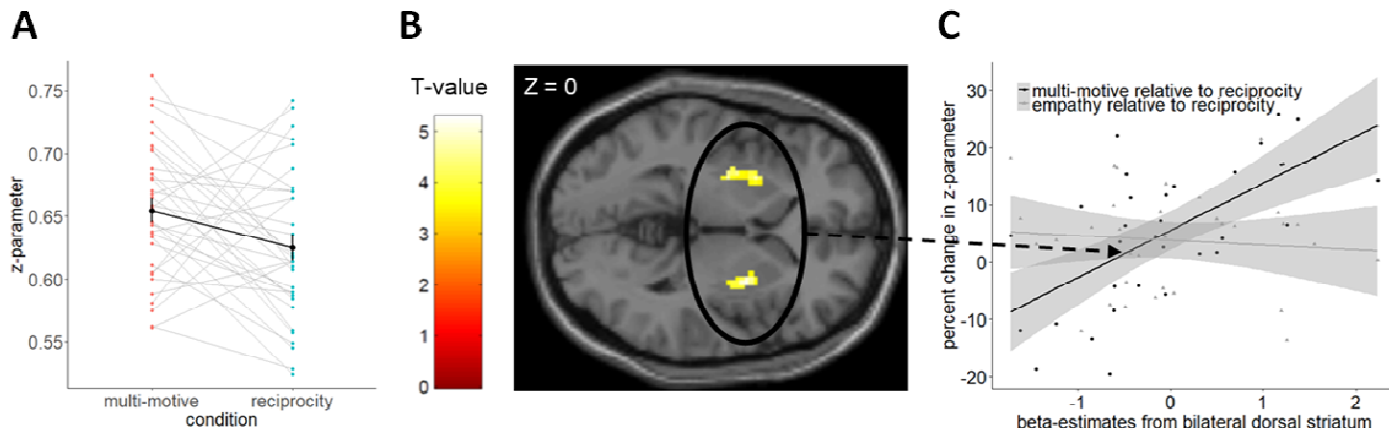

Figure 2. Increase in initial prosocial choice preferences in the multi-motive condition relative to the reciprocity condition and related neural activity. **(A)** Initial prosocial choice preferences (*z*-parameter) were significantly stronger in the multi-motive compared to the reciprocity condition ($\chi^2 = 4.78$, P = .03). Individual values are depicted in red (multi-motive condition) and in blue (reciprocity condition), means, and standard errors of the mean are depicted in black. **(B)** The individual changes of initial prosocial choice preferences in the multi-motive condition relative to the reciprocity condition were tracked by an increase in neural responses in the bilateral dorsal striatum ($P(FWE_{cluster\text{-}corrected}) = .018$; MNI peak coordinates; right hemisphere: x = 30, y = 2, z = -2, left hemisphere: x = -28, y = 7, z = 1; visualized at P < .001 uncorrected; Table 1). **(C)** Visualization of the linear regression model with extracted beta-values from the bilateral dorsal striatum as the dependent variable. The results show that the individual increase in dorso-striatal activity was significantly correlated with changes of the initial prosocial choice preference (*z*-parameter) in the multi-motive condition relative to the reciprocity condition, but not with the relative difference between the empathy and reciprocity motives (see **Table S2** for the whole-brain analysis).

Taken together, the DDM results showed that the combination of the two motives enhanced participants' initial preferences for choosing the prosocial option, relative to the initial prosocial preferences induced by the reciprocity motive (captured by the percent change in the *z*-parameter). The combination of empathy and reciprocity also increased the amount of information that people used to make a choice relative to the reciprocity motive, and, with a similar trend also relative to empathy (captured by the percent change in the *a*-parameter). In contrast, the speed of information accumulation, i.e., the efficiency of the choice process itself, was comparable between multi-motive and single-motive conditions (no change in *v*-parameter).

It is possible that the observed percent changes in the multi-motive condition relative to the reciprocity condition (in the *z*- and the *a*-parameters) originate from an interplay between the two motives when simultaneously activated in the multi-motive condition. However, as we observed no significant difference between the multi-motive condition and the empathy-condition, it is also conceivable that the empathy motive replaced the reciprocity motive when the two motives were activated simultaneously. In this case, the observed percent changes in the multi-motive condition would reflect the dominance of empathy over reciprocity, instead of an interplay between the two

motives. If empathy replaced the co-activated reciprocity motive, the relative difference in the *z*-parameters and *a*-parameters between the empathy and the reciprocity conditions should predict the individual extent of the percent changes in the multi-motive condition relative to the reciprocity condition. To test this, we calculated the relative differences in the *z*-parameters and *a*-parameters between empathy and reciprocity ($\Delta z_{\text{empathy/reciprocity}} = \frac{z_{\text{empathy}} - z_{\text{reciprocity}}}{z_{\text{reciprocity}}} \times 100$ and $\Delta a_{\text{empathy/reciprocity}} = \frac{a_{\text{empathy}} - a_{\text{reciprocity}}}{a_{\text{reciprocity}}} \times 100$), entered them as predictors in a regression analysis, and tested their effects on the observed percent changes in the multi-motive condition ($\Delta z_{\text{multi-motive/reciprocity}}$; $\Delta a_{\text{multi-motive/reciprocity}}$). This analysis revealed no significant effects ($\beta = 0.11$, $P = .55$; interaction with parameter type (*z* vs *a*): $\beta = -0.02$, $P = .93$). These results demonstrated that the difference between the two motives cannot account for the changes in choice parameters in the multi-motive condition relative to the reciprocity condition, bolstering the claim that the multi-motive effects observed reflect an interplay between the two motives.

Next, we investigated how the interplay between the two motives, and the resulting changes in initial prosocial preferences and amount of information affected the neural computation of prosocial choices. To do so, we regressed participants' individual percent change in initial prosocial preferences ($\Delta z_{\text{multi-motive/reciprocity}}$) and the amount of information ($\Delta a_{\text{multi-motive/reciprocity}}$) on the neural contrast in prosocial choices between the multi-motive condition and the reciprocity condition, using second-level regression. As a main result, the first analysis revealed activations in the bilateral dorsal striatum that were related to the individual change in prosocial preferences ($P(FWE_{\text{cluster-corrected}}) = 0.018$; center co-ordinates: x = 30, y = 2, z = -2; x = -28, y = 7, z = 1; **Fig. 2B, Table 1**). The stronger the percent increase in initial prosocial preferences in the multi-motive condition relative the reciprocity condition, the stronger the neural response in bilateral dorsal striatum.

Table 1. Neural results of the second-level regression between prosocial choice-related activity in the multi-motive condition > reciprocity condition and increase in prosocial choice preferences in the multi-motive condition relative to reciprocity ($\Delta z_{\text{multi-motive/reciprocity}}$) (P < .001 uncorrected, k > 10 voxels).

Region	Hemisphere	x y z	Cluster size	*t*-value	P($FWE_{\text{cluster-corrected}}$)
Putamen	Right	30 2 -2	85	5.24	.018
	Left	-28 7 1	84	4.77	.019
Middle cingulate gyrus	Right	8 -24 31	26	5.30	.524
Posterior cingulate gyrus	Right	8 -39 21	23	4.45	.611
Precentral gyrus	Left	-58 -1 16	22	4.22	.641
Hippocampus	Right	-23 -16 -22	15	4.00	.851
	Left	28 -11 -15	12	3.81	.922

The respective second-level regression with the percent change in the *a*-parameter revealed neural activity in the left anterior insula on a lower, uncorrected threshold (**Table S1**).

Again, we tested the alternative hypothesis that the increase in dorso-striatal activity may reflect the dominance of empathy (captured by the relative difference in *z*-parameters between empathy and reciprocity, $\Delta z_{\text{empathy/ reciprocity}}$), instead of an interplay between the motives. We extracted the individual beta estimates from the observed bilateral dorsal-striatum cluster (**Fig. 2B**; using the entire clusters in both hemispheres) for use as a dependent variable in a linear regression. The predictors were the percent change in *z*-parameters ($\Delta z_{\text{multi-motive/reciprocity}}$) and the relative empathy vs reciprocity difference ($\Delta z_{\text{empathy/ reciprocity}}$). The results showed a significant relationship between the individual increase in dorso-striatal activity and the percent change in the multi-motive condition relative to the reciprocity condition ($\Delta z_{\text{multi-motive/reciprocity}}$ β = .65, P = .00003), but not between neural activity and the difference in the *z*-parameters between the empathy and reciprocity conditions ($\Delta z_{\text{empathy/reciprocity}}$ β = -.15, P = .28) (**Fig. 2C**).

We also conducted a whole-brain analysis that compared the effect of $\Delta z_{\text{multi-motive/reciprocity}}$ and the effect of $\Delta z_{\text{empathy/reciprocity}}$ on the neural multi-motive vs reciprocity contrast. Supporting the results shown in **Fig. 2C**, we found stronger dorsal striatal activity for the whole-brain regression with $\Delta z_{\text{multi-motive/reciprocity}}$ compared to $\Delta z_{\text{empathy/reciprocity}}$ (**Table S2**). Together, these results showed that neural responses in the bilateral dorsal striatum tracked the changes in initial prosocial preferences in the multi-motive condition relative to the reciprocity condition, but not differences in initial prosocial preferences between the single-motive conditions.

We conducted a final analysis to specify the mechanism through which the multi-motive induced changes in initial prosocial preferences in the dorsal striatum affect the actual frequency of prosocial choices. According to one possible multi-motive choice model, the neural change in initial prosocial preferences may have a direct effect on the frequency of prosocial choices, i.e., it may directly predict the observed enhancement of prosocial choices in the multi-motive condition compared to the reciprocity condition. Alternatively, it may affect prosocial choices indirectly via its impact on the amount of processed information, i.e., the other parameter that was enhanced in the multi-motive condition ($\Delta a_{\text{multi-motive/ reciprocity}}$). The hypothesis of an indirect model is inspired by the observed significant negative correlation between the individual percent changes in the *z*-parameter and the *a*-parameter ($\Delta z_{\text{multi-motive/reciprocity}}$; $\Delta a_{\text{multi-motive/ reciprocity}}$) (*rho* = -.61, P = .0002).

We conducted path analyses (Rosseel, 2012) to test these two alternative models. The individual beta-estimates of initial prosocial preference-related activity in the bilateral dorsal striatum were used as predictor variables. The individual percent changes in the amount of information ($\Delta a_{\text{combined/reciprocity}}$) served as the mediator, and the percent change in prosocial choices in the multi-motive condition relative to the reciprocity condition ($\Delta prosoc_{\text{multi-motive/reciprocity}}$) was entered as the dependent variable (**Fig. 3**). The results revealed significant indirect paths (standardized path a coefficient = -.47, P = .002; standardized path b coefficient = -.23, P = .021), but no significant direct effect (standardized path c coefficient = -.15, P = .294). These results indicated that individual neural changes in initial prosocial preferences affect prosocial choices indirectly via their impact on the amount of information that people consider while making a choice. The negative relationship between initial prosocial preferences in the dorsal striatum and the amount of processed information (the negative coefficient of path a) showed that an increase in initial prosocial preferences reduced the amount of information that was processed to reach a prosocial choice, i.e., enhanced selectivity in

information processing. This enhancement in processing selectivity, in turn, increased the frequency of prosocial choices (the negative coefficient of path b).

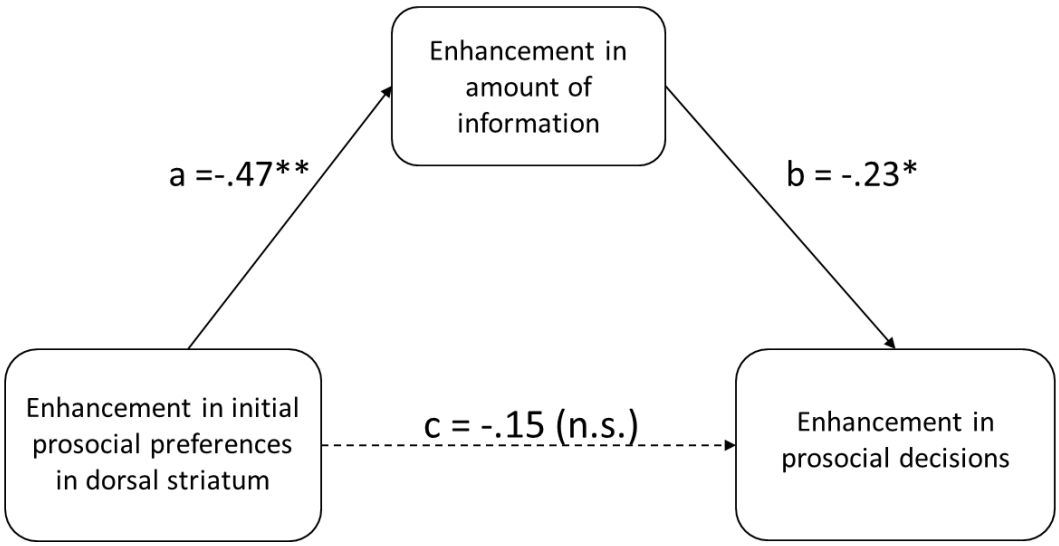

Figure 3. Path model results. The percent change of initial prosocial preferences in the multi-motive condition relative to the reciprocity condition in the dorsal striatum was used as the predictor variable. The percent change of the amount of information in the multi-motive condition relative to the reciprocity condition served as the mediator and the percent change in prosocial choices in the multi-motive condition relative to the reciprocity condition was entered as the dependent variable. The results indicate that the individual neural changes in initial prosocial choice preferences affect prosocial choices indirectly by decreasing the amount of information that participants considered to reach the prosocial choice boundary. **P < .01, *P < .05

Discussion

Many behaviors derive from complex motivational states that are characterized by different, simultaneously activated motives (Engel & Zhurakhovska, 2016; Hughes & Zaki, 2015; Jagers et al., 2017; Takeuchi et al., 2015; Terlecki & Buckner, 2015). However, the mechanisms through which interacting motives affect behaviors, e.g., the computation of social choices, are poorly understood. Our findings provide such a mechanism. We show that multiple social motives, per se, impede the choice process because people consider more information to reach the threshold for one choice option. However, counteracting this overflow in information, the interplay between different motives biases individuals' initial preferences towards one choice option, in our case the prosocial choice. According to this model, a complex motivational state (characterized by more than one motive) can facilitate the individual choice process compared to a simple motivational state by sharpening individual choice preferences.

The change in individual choice preferences in complex motivational states was tracked by the neural response in bilateral dorsal striatum. That is, neural activation in dorsal striatum correlated with changes in initial choices preferences in the multi-motive condition relative to the reciprocity condition (see **Fig. 2B)**, and on a lower threshold (P uncorrected < 0.005), also relative to the empathy condition (**Fig. S1)**. The latter shows that the dorsal striatum captured the difference in initial choice preferences between the multi-motive condition and the empathy condition, despite the lack of significant behavioral differences. In contrast, the dorsal striatum did not process the difference in initial choice preferences between the individual motives (**Fig. 2C; Table S2**).

Previous studies have shown that the striatum supports the transfer of motivation (e.g., elicited by rewards) to goal-directed behaviors (Báez-Mendoza & Schultz, 2013; Bhanji & Delgado, 2014; Burton, Nakamura, & Roesch, 2015; Kim & Im, 2018; Salamone et al., 2016; Shohamy, 2011; Wang et al., 2013). Extending this previous evidence, we show that the dorsal striatum integrates choice preferences that are elicited by different motivational forces. Thus, it provides a neural hub through which complex motivational states are generated and implemented in behavior.

We found that the simultaneous activation of the two motives in the multi-motive condition enhanced the participants' initial prosocial preferences relative to the reciprocity condition. This indicates that the empathy motive enhanced the reciprocity motive, but not vice versa. Given this result, we argued that the observed changes in the multi-motive condition may reflect the dominance of one motive over the other motive (i.e., a dominance of empathy over reciprocity). If this were true, the multi-motive induced changes in the choice process would reflect a motivation that is similar to the state induced by the dominant motive, instead of a novel motivational state that was incited by the interplay between different motives. Our results show that the multi-motive induced changes in the choice process (i.e., DDM and neural choice parameters) are related to differences between the multi-motive condition and the reciprocity condition, and cannot be explained by differences between the empathy and the reciprocity motive. This finding supports the conclusion that the simultaneous activation of two motives elicits a novel motivational state that stems from the interplay between the different motives.

The combination of the two motives yielded these changes in the choice process, even though the participants perceived the two motives as equally strong and both motives increased the frequency of prosocial choices to the same extent (based on their comparable induction ratings and their association with the frequency of prosocial choices in both single-motive conditions). We obtained our

findings with a paradigm that directly compared the computation of prosocial choices in a person who is in a complex motivational state (i.e., driven by several motives at the same time) and computation of choices in this same person when only one motive was active. Thus, our results provide a model that specifies how prosocial choices are computed based on multiple motives, compared to a single motive. According to this model, the interplay between different social motives alters the preferences with which a person enters the prosocial choice process, tracked by an increased neural response in dorsal striatum. This increase in dorso-striatal activity, in turn, enhances the selectivity of information processing. Together, our findings provide a plausible neurobiological model for human goal-directed behavior in complex motivational states, a phenomenon that is widely observed (Kruglanski et al., 2018; Lewin et al., 1951), but has so far not been explained.

Materials and Methods

Experimental model and subject details

The objective of our study was to compare the computation of a goal-directed behavior in a complex motivational state (i.e., driven by simultaneously activated multiple motives), with the computation of this same behavior in a simple motivational state (i.e., only driven by one specific motive). To achieve this objective we used a within-subject design in which each participant performed the identical social choice task under four different conditions: a multi-motive condition in which two motives were activated simultaneously, two single-motive conditions in which each of the two motives was activated separately, and a control condition without motive activation. Forty-two right-handed healthy female participants (mean age = 23.1 years, SD = 2.8 years) and four female confederates took part in the experiment. We chose female participants as well as female confederates in order to control for gender and avoid cross-gender effects. The confederates were students who had been trained to serve in all the different conditions counterbalanced across participants. Prior to the experiment, written informed consent was obtained from all the participants. The study was approved by the local ethics committee (BB 023/17). Participants received monetary compensation. Four participants had to be excluded due to technical problems and excessive head movements, five participants had to be excluded as outlier based on their choices (less than ten prosocial choices across all condition; three standard deviations above the mean). Thus, we analyzed 33 data sets using a within-subjects design.

Method details

Procedure

Prior to the task, the individual thresholds for pain stimulation were determined for the participants and all the confederates. Next, the participants and confederates were assigned to their different roles by a manipulated lottery (drawing matches). In order to ensure that each participant was always assigned her designated role as a participant (pain recipient during motive induction; decider during the decision task), the drawing of the matches was organized in such a way that she always drew the last match. The confederates were assigned to the roles of the empathy partner, the reciprocity partner, the multi-motive partner, or the baseline partner, counterbalanced across participants.

In accordance with these roles, two of the confederates first went to an ostensible other experiment and the other two waited to be seated in the scanner room. Each confederate was matched with a specific color and seating position (to the left vs. to the right of the fMRI scanner), with her color designation and seating position counter-balanced across participants.

During scanning, two confederates (the empathy partner, reciprocity partner, multi-motive partner, or baseline partner) were seated to the left and the right of the participant who was lying inside the fMRI scanner, and the participants allocated points to their respective partners. The order of motive induction and the type of partner the confederates represented were counter-balanced across participants.

At the end of the experiment, all the confederates left and the participants stayed in the scanner until anatomical image acquisition was completed. Finally, participants were asked to complete a questionnaire measuring trait aspects of empathy (Jordan, Amir, & Bloom, 2016). Participants spent approximately 60 min in the scanner and the entire procedure lasted about 2.5 hours. To avoid possible reputation effects, which could influence participants' behavior, participants were informed that they would not meet the confederates after the experiment.

Empathy induction

Each empathy-induction trial started with a colored arrow shown for 1,000 ms, which indicated the empathy partner. After this cue and a jittered (1,000–2,000 ms) fixation cross, the same colored flash was displayed for 1,500 ms. Participants were informed that a dark-colored flash indicated that the corresponding partner received a painful stimulus at that moment; a light-colored flash indicated a non-painful stimulus. Next, the rating scale was shown for a maximum of 6 s. Participants reported how they felt after observing the partner receive painful or non-painful stimuli ("*How do you feel?*" in German). The scale ranged from -4 (labeled "*very bad*") to +4 (labeled "*very good*") and was visually

displayed in steps of 1. Before analysis, the induction ratings were recoded such that high positive values reflect strong responses to the induction procedure (strong empathy motive). Participants had to respond within 6 s. The inter-trial interval was 1,500 ms. Empathy induction consisted of 12 trials: nine that were ostensibly painful for their partner (i.e., the confederate).

Reciprocity induction

Each reciprocity-induction trial also started with an arrow colored in the reciprocity partner's color, which pointed toward the seating position of the reciprocity partner (left or right) and was shown for 1,000 ms. Next, the participants were shown a flash displayed to the right and a crossed-out flash displayed to the left of a centered fixation cross. Participants were told that this was the decision screen, which the reciprocity partner also saw while making her decision to either save or not save the participant from painful stimulation. After a jittered interval of 2,000 to 4,000 ms, a box appeared around one of the flashes, indicating the ostensible choice of the reciprocity partner. Depending on where the box was displayed, the reciprocity partner had either decided to forego a monetary award of 2 € in order to save the participant from painful stimulation (a box around the crossed-out flash) or decided to take the money and not save the participant (a box around the flash that was not crossed-out).

After an additional 1,000 ms, the rating scale appeared asking the participant to indicate how she felt having just observed that the reciprocity partner decided to save or not save her from painful stimulation ("*How do you feel?*" in German). The rating scale was identical in all the types of induction trials. Before analysis, the induction ratings were recoded such that high positive values reflect strong responses to the induction procedure (strong reciprocity motive).

After a jittered (1,000 to 2,000 ms) fixation cross, the participant was informed whether the decision of the reciprocity partner would be implemented ("*decision accepted*") or not ("*decision declined*"). This information was displayed for 1,000 ms. This additional stage was included in order to ensure the same amount of painful stimulations across all conditions (50 %), while at the same time allowing for the high rate (75%; 9 out of 12 trials; see[3]) of the reciprocity partner's decisions to help.

Thus, four types of reciprocity trials were possible. When the partner decided to save the participant from painful stimulation and this decision was accepted, the participant did not receive a painful stimulus, which was visually represented by a crossed-out flash (1,500 ms). However, when the reciprocity partner's decision to save the participant was declined, participants received a painful stimulus, which was accompanied by the display of a flash (1,500 ms). Similarly, when the partner

decided not to save the participant and this decision was accepted, the participant received a painful stimulus accompanied by the display of a flash. Finally, when the partner decided to not save the participant and this decision was declined, the participant did not receive painful stimulation, which was visually represented by a crossed-out flash. The inter trial fixation cross was displayed for 1,500 ms before the next trial started.

Multi-motive induction

The multi-motive induction procedure combined the empathy- and reciprocity-induction procedures. As in the empathy-induction condition, it included 12 empathy induction trials, nine ostensibly painful for the partner. As in the reciprocity-induction condition, it included 12 reciprocity trials and participants received help in nine out of 12 trials. The stimulation and trial structure were identical to the empathy- and reciprocity-induction trials, except that the relevant colors were replaced by the colors matched to the multi-motive partner (i.e., the color of the pain flash in the empathy trials and the color of the box highlighting the decision of the partner in the reciprocity trials).

Additional control trials for empathy and reciprocity induction

In order to equalize the number and types of trials (i.e., the length and structure of the interaction with each motive partner) across conditions, the empathy-induction procedure also included trials that were identical to the reciprocity trials, except that the computer decided whether the participant would be saved from a painful stimulus and not the empathy partner. This computer's decision was visually represented by a white-colored box appearing either around the crossed-out flash (saving the participant) or the normal flash (not saving the participant). It was clearly explained to each participant that the color white was not matched with any of the partners but indicated the computer's choice. The empathy-induction procedure consisted of 12 control trials, in addition to the 12 empathy trials described above, resulting in 24 trials, i.e., the identical number of trials as the multi-motive induction procedure.

Similarly, the reciprocity-induction procedure included trials that were identical to the empathy-induction trials, except that the reciprocity partner only received non-painful stimulation on these trials, as visually represented by a light-colored flash. In total, the reciprocity-induction procedure consisted of 12 of these control trials and 12 reciprocity trials (see above), i.e., 24 trials (identical to the other conditions).

Baseline induction

The baseline procedure consisted of 24 trials in total, 12 trials in which the baseline partner only received non-painful stimulation and 12 trials in which the computer decided whether the participant would be saved from a painful stimulus or not. This computer's decision was visually represented by a white-colored box either appearing around the crossed-out flash (saving the participant) or the normal flash (not saving the participant). It was clearly explained to the participant that the white box did not represent the decision of a person, but indicated the computer's choice.

Pain stimulator

For pain stimulation, we used a mechano-tactile stimulus generated by a small plastic cylinder (513 g). The projectile was shot against the cuticle of the left index finger using air pressure (Impact Stimulator, Labortechnik Franken, Release 1.0.0.34). The criterion for painful stimulation was a subjective value of 8 on a pain scale ranging from 1 (no pain at all, but a participant could feel a slight touch of the projectile) to 10 (extreme, hardly bearable pain). The participants were told that a value of 8 corresponded to a painful, but bearable stimulus, and a non-painful stimulus corresponded to a value of 1 on the same subjective pain scale. These subjective pain thresholds were determined using a stepwise increase of air pressure (stepsize of 0.25 mg/s), starting with the lowest possible pressure (0.25 mg/s), which caused the projectile to barely touch the cuticle, and increasing in stimulus intensity until it reached a level that corresponded to the individual's value of 8 (range = 2.75–3.5 mg/s).

Choice task

The choice task was identical in all the conditions. Participants were asked to repeatedly choose between two different distributions of points that each represented different amounts of monetary pay-offs for themselves and one of the partners (see **Fig. 1A**). Each choice-trial started with a colored arrow shown for 1,000 ms, indicating the next interaction partner. After this cue, participants saw the two possible distributions of points in different colors, indicating the potential gain for the participant or the potential gain for the current partner. Participants had to choose one of the distributions within 4,000 ms. A green box appeared around the distribution that was selected by the participant at 4,000 ms after distribution onset. The box was shown for 1,000 ms. The length of the inter-trial interval, as indicated by a fixation cross, was jittered between 4,000 and 6,000 ms. At the end of the experiment, two of the distributions chosen by the participant were randomly selected for payment (100 points = 50 cents). Participants performed 42 choice trials in each motive-induction condition, i.e., 168 trials in total.

Quantification and statistical analyses

Regression analyses

Regression analyses were conducted using the R-packages “lme4 and “car” (R Core-Team, 2018). The frequency of prosocial choices was calculated for each participant for each condition (empathy, reciprocity, multi-motive, and baseline) and entered as a dependent variable into a linear mixed model (lmm) with conditions as fixed effects (empathy, reciprocity, multi-motive, and baseline) and participants as random effects. To investigate the differences between the social motives more closely, additional lmm analyses were conducted that only included the multi-motive condition and the reciprocity or the empathy condition as fixed effects and participants as random effects. Parallel analyses were conducted for reaction times and the DDM parameters *v*, *z*, and *a*.

To test whether the relative difference between empathy and reciprocity on the *z*-parameter and *a*-parameter could explain the percent changes of these parameters in the multi-motive condition compared to the reciprocity condition, the percent change values ($\Delta z_{\text{multi-motive/reciprocity}}$ and $\Delta a_{\text{multi-motive/reciprocity}}$) were entered as dependent variables in a linear regression model. The respective relative differences ($\Delta z_{\text{empathy/reciprocity}}$ and $\Delta a_{\text{empathy/reciprocity}}$) and one regressor modeling the parameter type (*z*-parameter, *a*-parameter) were included as predictors.

To test whether the relative difference between empathy and reciprocity on the *z*-parameter could explain the effect in dorsal striatum, beta estimates from the neural contrasts between the multi-motive reciprocity conditions in the bilateral dorsal striatum were entered as the dependent variable, and $\Delta z_{\text{multi-motive/reciprocity}}$ and $\Delta z_{\text{empathy/reciprocity}}$ were entered as predictor variables.

Drift-Diffusion Modeling

We used hierarchical drift-diffusion modeling (HDDM (Vandekerckhove et al., 2011; Wiecki et al., 2013)), which is a version of the classical drift-diffusion model that exploits between-subject and within-subject variability using Bayesian parameter estimation methods, because it is ideal for use with relatively small sample sizes. The analyses were conducted using the python implementation of HDDM (Wiecki et al., 2013). Model comparisons using the deviance information criterion (DIC) showed that models that allowed for trial-by-trial variation in the drift rate, *v*, the non-decision time, *t*, the initial decision preference, *z*, and the amount of processed information, *a,* yielded the best model fit (i.e., lowest DIC value). Model convergence was checked by visual inspection of the estimation chain of the posteriors, as well as computing the Gelman-Rubin Geweke statistic for convergence (all values < 1.01) (Gelman & Rubin, 1992). Parameters of interest from the best-fitting model were

extracted for further analysis. Specifically, for each participant, the condition-specific *v*-parameters, *z*-parameters, and *a*-parameters were extracted (resulting in 12 parameters per participant).

In the next step, the parameters were entered as dependent variables in lmms, with conditions as fixed effects and participants as random effects (one model per parameter). For closer investigation of the effects between the social motives, additional lmm analyses were conducted that only included the multi-motive condition and the reciprocity condition or the empathy conditions as fixed effects and participants as random effects.

fMRI data acquisition

We used a 3T MRI-scanner (Verio, Siemens, Erlangen, Germany) with a 32-channel head coil. Functional imaging was performed with a multiband EPI sequence of 72 transversal slices oriented along the subjects' AC-PC plane (multi-band acceleration factor of 6). The in plane resolution was 2.5 x 2.5 mm^2 and the slice thickness was 2.5 mm. The field of view was 210 x 210 mm^2, corresponding to an acquisition matrix of 84 x 84. The repetition time was 1 s, the echo time was 33.6 ms, and the flip angle was 54°. Structural imaging was conducted using a sagittal T1-weighted 3D MPRAGE with 176 slices, and a spatial resolution of 1 x 1 x 1 mm^3. The field of view was 250 x 250 mm^2, corresponding to an acquisition matrix of 256 x 256. The repetition time was 1,690 ms, the echo time was 2.52 ms, the total acquisition time was 3:50 min, and the flip angle was 9°. For the T1-weighted images, GRAPPA with a PAT factor of 2 was used. We obtained, on average, 1,911 (SD = 5.6 volumes) EPI-volumes during the choice task of each participant. We used a rubber foam head restraint to avoid head movements.

Preprocessing

Preprocessing and statistical parametric mapping were performed with SPM12 (Wellcome Department of Neuroscience, London, UK) and Matlab version 9.2 (MathWorks Inc; Natick, MA). Spatial preprocessing included realignment to the first scan, and unwarping and coregistration to the T1 anatomical volume images. Unwarping of geometrically distorted EPIs was performed using the FieldMap Toolbox. T1-weighted images were segmented to localize grey and white matter, and cerebro-spinal fluid. This segmentation was the basis for the creation of a DARTEL Template and spatial normalization to Montreal Neurological Institute (MNI) space, including smoothing with a 6 mm (full width at half maximum) Gaussian Kernel filter to improve the signal-to-noise-ratio. To correct for low-frequency components, a high-pass filter with a cut-off of 128 s was used.

fMRI statistical analysis

Since our study focused on the effects of the different motive conditions on the prosocial choice process, fMRI analysis focused on those trials in which the participants made a prosocial choice.

First-level analyses were performed with the general linear model (GLM), using a canonical hemodynamic response function (HRF) and its first derivative (time derivative). Regressors were defined from cue onset until the individual response was made by pressing a button (resulting in a time window of 1,000 ms + individual response time). For each of the four conditions (the three motive conditions and baseline condition), the respective regressors of prosocial choice trials were included as regressors of interest. The respective regressors of all the other trials (e.g., egoistic choice trials and trials with missed button presses) were included as regressors of no interest. The residual effects of head motions were corrected by including the six estimated motion parameters for each participant and each session as regressors of no interest. To allow for modeling all the conditions in one GLM, an additional regressor of no interest was included, which modeled the potential effects of session.
For the second-level analyses, contrast images for comparisons of interest (empathy > reciprocity, multi-motive > empathy, reciprocity > empathy, and multi-motive > reciprocity) were initially computed on a single-subject level. In the next step, the individual images of the main contrast of interest (multi-motive > reciprocity) were regressed against the percent change in the *z*-parameter ($\Delta z_{\text{multi-motive/reciprocity}}$) and *a*-parameter ($\Delta a_{\text{multi-motive/reciprocity}}$) in the multi-motive condition, relative to the reciprocity condition, using second-level regressions. To test if the neural response in the dorsal striatum was related to the relative difference in *z* between empathy and reciprocity ($\Delta z_{\text{empathy/reciprocity}}$), the (multi-motive > reciprocity) contrast was regressed against the empathy vs reciprocity *z*-differences ($\Delta z_{\text{empathy/reciprocity}}$) and the multi-motive z-enhancement ($\Delta z_{\text{multi-motive/reciprocity}}$) in the same model. The individual beta-estimates of the neural multi-motive condition > reciprocity contrast were extracted from the bilateral clusters in the dorsal striatum resulting from the second-level regression with $\Delta z_{\text{multi-motive/reciprocity}}$ at a cluster-forming threshold of $P < .001$ uncorrected, using MarsBaR(Brett, Anton, Valabregue, & Poline, 2002).

The reported anatomical regions were identified using the xjView toolbox (http://www.alivelearn.net/xjview).

Path analysis

For the path analysis, we used the R-package lavaan (Rosseel, 2012). We entered the beta-estimates that were extracted from the bilateral putamen clusters that we obtained from the second-

level regression with $\Delta z_{\text{multi-motive/reciprocity}}$ as predictor variables, $\Delta a_{\text{multi-motive/reciprocity}}$ as the mediator and $\Delta prosoc_{\text{multi-motive/reciprocity}}$ as the dependent variable. Trait empathy (the Empathy subscale of the extended IRI) (Jordan et al., 2016) and relative motive strength, as captured by the difference in induction ratings between the multi-motive and the reciprocity motive condition ($\text{ratings}_{\text{multi-motive}}$-$\text{ratings}_{\text{reciprocity}}$), were included as control variables.

Data and code availability

Behavioral data and scripts are available at github.com:

https://github.com/AnneSaulin/complex_motivations

Imaging data are available at neurovault.org:

https://www.neurovault.org/collections/5879/

Acknowledgments

We thank Martin Domin, Jörg Pfannmöller, and Kai Klepzig for their technical support, and Vassil Iotzov for helpful discussions about the data. This study was supported by the German Research Foundation (HE 4566/2-1; HE 4566/5-1) and the German Academic Scholarship Foundation.

Author Contributions

G.H. and A.S. designed the research with input from J.K., M.L., and U.H.; A.S. and U.H. performed the research; A.S. programmed the experiment; A.S. and U.H. analyzed the data with input from G.H., M.L., and J.K.; G.H. and A.S. wrote the paper with input from U.H., M.L., and J.K..

Competing interests

The authors declare no competing interests.

References

Báez-Mendoza, R., & Schultz, W. (2013). The role of the striatum in social behavior. *Frontiers in Neuroscience*, *7*(233). https://doi.org/10.3389/fnins.2013.00233

Batson, C. D., Ahmad, N., & Stocks, E. L. (2011). Four forms of prosocial motivation egoism, altruism, collectivism, and principlism. In D. Dunning (Ed.), *Social Motivation* (pp. 103–126). New York: Psychology Press. https://doi.org/10.4324/9780203833995

Batson, C. D., Turk, C. L., Shaw, L. L., & Klein, T. R. (1995). Information Function of Empathic Emotion. *Journal of Personality and Social Psychology*, *68*(February), 300–313.

Bhanji, J. P., & Delgado, M. R. (2014). The social brain and reward: Social information processing in the human striatum. *Wiley Interdisciplinary Reviews: Cognitive Science*, *5*(1), 61–73. https://doi.org/10.1002/wcs.1266

Brett, M., Anton, J. L., Valabregue, R., & Poline, J. B. (2002). Region of interest analysis using an SPM toolbox - abstract presented at the 8th International Conference on Functional Mapping of the Human Brain, June 2-6, 2002, Sendai, Japan. *NeuroImage*. https://doi.org/http://dx.doi.org/10.1016/S1053-8119(02)90010-8

Burton, A. C., Nakamura, K., & Roesch, M. R. (2015). From ventral-medial to dorsal-lateral striatum: Neural correlates of reward-guided decision-making. *Neurobiology of Learning and Memory*, *1*(117), 51–59. https://doi.org/10.1016/j.nlm.2014.05.003

Chen, F., & Krajbich, I. (2018). Biased sequential sampling underlies the effects of time pressure and delay in social decision making. *Nature Communications*, *9*(1), 1–10. https://doi.org/10.1038/s41467-018-05994-9

Cromwell, H. C., & Schultz, W. (2006). Effects of Expectations for Different Reward Magnitudes on Neuronal Activity in Primate Striatum. *Journal of Neurophysiology*, *89*(5), 2823–2838. https://doi.org/10.1152/jn.01014.2002

Engel, C., & Zhurakhovska, L. (2016). When is the risk of cooperation worth taking? The prisoner's dilemma as a game of multiple motives. *Applied Economics Letters*, *23*(16), 1157–1161. https://doi.org/10.1080/13504851.2016.1139672

Flagan, T., Mumford, J. A., & Beer, J. S. (2017). How do you see me? The neural basis of motivated meta-perception. *Journal of Cognitive Neuroscience*, *29*(11), 1908–1917. https://doi.org/10.1162/jocn_a_01169

Forstmann, B. U., Ratcliff, R., & Wagenmakers, E.-J. (2016). Sequential Sampling Models in Cognitive Neuroscience: Advantages, Applications, and Extensions. *Annual Review of Psychology*, *67*. https://doi.org/10.1146/annurev-psych-122414-033645

Gelman, A., & Rubin, D. B. (1992). Inference from Iterative Simulation Using Multiple Sequences. *Statistical Science*, *7*(4), 457–472.

Gouldner, A. W. (1960). The Norm of Reciprocity: A Preliminary Statement. *American Sociological Review*. https://doi.org/10.2307/2092623

Hein, G., Morishima, Y., Leiberg, S., Sul, S., & Fehr, E. (2016). The brain's functional network architecture reveals human motives. *Science*, *351*(6277), 1074–1078.

Hughes, B. L., & Zaki, J. (2015). The neuroscience of motivated cognition. *Trends in Cognitive Sciences*, *19*(2), 62–64. https://doi.org/10.1016/j.tics.2014.12.006

Jagers, S. C., Linde, S., Martinsson, J., & Matti, S. (2017). Testing the Importance of Individuals' Motives for Explaining Environmentally Significant Behavior. *Social Science Quarterly*, *98*(2), 644–658. https://doi.org/10.1111/ssqu.12321

Janczyk, M., & Lerche, V. (2019). A diffusion model analysis of the response-effect compatibility effect. *Journal of Experimental Psychology: General*, *148*(2), 237–251.

Jennings, J. H., Sparta, D. R., Stamatakis, A. M., Ung, R. L., Pleil, K. E., Kash, T. L., & Stuber, G. D. (2013). Distinct extended amygdala circuits for divergent motivational states. *Nature*, *496*(7444), 224. https://doi.org/10.1038/nature12041

Jordan, M. R., Amir, D., & Bloom, P. (2016). Are empathy and concern psychologically distinct? *Emotion*, *16*(8), 1107–1116. https://doi.org/10.1037/emo0000228

Kennedy, P. J., & Shapiro, M. L. (2009). Motivational states activate distinct hippocampal representations to guide goal-directed behaviors. *Proceedings of the National Academy of Sciences*. https://doi.org/10.1073/pnas.0903259106

Kim, B., & Im, H.-I. (2018). The role of the dorsal striatum in choice impulsivity. *Annals of the New York Academy of Sciences*.

Krajbich, I., Hare, T., Bartling, B., Morishima, Y., & Fehr, E. (2015). A Common Mechanism Underlying Food Choice and Social Decisions. *PLoS Computational Biology*. https://doi.org/10.1371/journal.pcbi.1004371

Kruglanski, A. W., Shah, J. Y., Fishbach, A., Friedman, R., Chun, W. Y., & Sleeth-Keppler, D. (2018).

A theory of goal systems. In *The motivated mind* (pp. 215–258). Routledge. https://doi.org/10.4324/9781315175867

Lamm, C., Decety, J., & Singer, T. (2011). Meta-analytic evidence for common and distinct neural networks associated with directly experienced pain and empathy for pain. *NeuroImage*, *54*(3), 2492–2502. https://doi.org/10.1016/j.neuroimage.2010.10.014

Lewin, K., Cartwright, D., & Price, D. (1951). *Field theory in social science: Selected theoretical papers.* (D. Cartwright, Ed.), *American Sociological Review*. https://doi.org/10.1037/0021-9010.69.1.85

McCabe, K. A., Rigdon, M. L., & Smith, V. L. (2003). Positive reciprocity and intentions in trust games. *Journal of Economic Behavior and Organization*, *52*(2), 267–275. https://doi.org/10.1016/S0167-2681(03)00003-9

Mulder, M. J., Wagenmakers, E.-J., Ratcliff, R., Boekel, W., & Forstmann, B. U. (2012). Bias in the Brain: A Diffusion Model Analysis of Prior Probability and Potential Payoff. *Journal of Neuroscience*, *32*(7), 2335–2343. https://doi.org/10.1523/jneurosci.4156-11.2012

Palmiter, R. D. (2008). Dopamine signaling in the dorsal striatum is essential for motivated behaviors: Lessons from dopamine-deficient mice. *Annals of the New York Academy of Sciences*, (1129), 35. https://doi.org/10.1196/annals.1417.003

Ratcliff, R., Smith, P. L., Brown, S. D., & McKoon, G. (2016). Diffusion Decision Model: Current Issues and History. *Trends in Cognitive Sciences*, *20*(4), 260–281. https://doi.org/10.1016/j.tics.2016.01.007

Robinson, S., Sotak, B. N., During, M. J., & Palmiter, R. D. (2006). Local dopamine production in the dorsal striatum restores goal-directed behavior in dopamine-deficient mice. *Behavioral Neuroscience*, *120*(1), 196. https://doi.org/10.1037/0735-7044.120.1.000

Rosseel, Y. (2012). **lavaan**: An *R* Package for Structural Equation Modeling. *Journal of Statistical Software*. https://doi.org/10.18637/jss.v048.i02

Salamone, J. D., & Correa, M. (2012). The Mysterious Motivational Functions of Mesolimbic Dopamine. *Neuron*, *76*(3), 470–485. https://doi.org/10.1016/j.neuron.2012.10.021

Salamone, J. D., Pardo, M., Yohn, S. E., López-Cruz, L., Sanmiguel, N., & Correa, M. (2016). Mesolimbic dopamine and the regulation of motivated behavior. In *Behavioral neuroscience of motivation* (pp. 231–257). Springer, Cham. https://doi.org/10.1007/7854_2015_383

Shohamy, D. (2011). Learning and motivation in the human striatum. *Current Opinion in Neurobiology*, *21*(3), 408–414. https://doi.org/10.1016/j.conb.2011.05.009

Takeuchi, R., Bolino, M. C., & Lin, C. C. (2015). Too many motives? The interactive effects of multiple motives on organizational citizenship behavior. *Journal of Applied Psychology*, *100*(4), 1239. https://doi.org/10.1037/apl0000001

Team, R. C. (2018). R: A Language and Environment for Statistical Computing.

Terlecki, M. A., & Buckner, J. D. (2015). Social anxiety and heavy situational drinking: Coping and conformity motives as multiple mediators. *Addictive Behaviors*, *40*, 77–83. https://doi.org/10.1016/j.addbeh.2014.09.008

Toelch, U., Panizza, F., & Heekeren, H. R. (2018). Norm compliance affects perceptual decisions through modulation of a starting point bias. *Royal Society Open Science*, *5*(3), 171268. https://doi.org/10.1098/rsos.171268

Vandekerckhove, J., Tuerlinckx, F., & Lee, M. D. (2011). Hierarchical Diffusion Models for Two-Choice Response Times. *Psychological Methods*, *16*(1), 44–62. https://doi.org/10.1037/a0021765

Wang, A. Y., Miura, K., & Uchida, N. (2013). The dorsomedial striatum encodes net expected return, critical for energizing performance vigor. *Nature Neuroscience*, *16*(5), 639. https://doi.org/10.1038/nn.3377

Wiecki, T. V., Sofer, I., & Frank, M. J. (2013). HDDM: Hierarchical Bayesian estimation of the Drift-Diffusion Model in Python. *Frontiers in Neuroinformatics*, *7*, 14. https://doi.org/10.3389/fninf.2013.00014